Nanostructuring of Semiconductors

G. Brunthaler, H. Straub, A. Darhuber, T. Grill, Y. Zhuang, E. Wirthl, H. Sitter, G. Bauer

Institut für Halbleiterphysik, Johannes Kepler Universität, A-4040 Linz, Austria

Periodic nanostructure patterns based on molecular epitaxy grown CdZnSe/ZnSe single quantum wells and Si/SiGe heterostructures have been defined by holographic lithography or electron beam lithography and fabricated by reactive ion etching. The CdZnSe/ZnSe structures exhibit photoluminescence emission down to the smallest investigated lateral width of 80 nm. For the narrow wires a spectral red shift of the photoluminescence emission up to 8 meV is observed which is explained by a partial elastic strain relaxation of the biaxial compressively strained CdZnSe quantum well layer after the patterning process. Detailed calculations of the inhomogeneous strain status and the piezoelectric effect of the partially relaxed wire structures and the resulting band gap changes were performed and compared with the experiment. The large area Si/SiGe periodic wire structures were investigated by high resolution x-ray diffraction.

1. Introduction

The realization of semiconductor nanostructures is relevant for future electronic devices, optical emitters and the investigation of basic physical properties. In II-VI semiconductors the realization of wide band-gap blue-green diode lasers [1], [2] initiated the interest in light emitters from nanostructures. In such a nanostructure it is expected that low threshold laser structures can be realized.

In Si/SiGe heterostructures the investigation of nanostructures is driven by the miniaturization of today's integrated circuits and the potential of the Si/SiGe material system to increase the performance of such devices. Both material systems mentioned consist of strained layers, and the investigation of strain relaxation effects due to the formation of laterally patterned nanostructures is needed for practical implementations.

The purpose of our Si/SiGe study was to find a reliable etching procedure for the fabrication of Si/SiGe sub-micron structures. There are previous reports in the literature that in particular the sidewall steepness of SiGe embedded in Si is much worse than that of silicon. The etched Si/SiGe structures were then structurally characterized by x-ray diffraction.

2. Sample preparation

The II-VI and Si/SiGe heterostructures were both grown by molecular beam epitaxy in Linz. The CdZnSe/ZnSe single quantum well (QW) heterostructures consist of a 1.1 µm thick, fully relaxed ZnSe buffer on top of the GaAs (001) substrate (grown by W. Faschinger). A 10 nm CdZnSe layer forms the QW and a 100 nm ZnSe layer acts as a cap. High density periodic patterns were defined either by holographic or electron beam lithography. In the case of e-beam lithography, well defined arrays of 40 x 40 μm^2 with

wires and dots of different lateral size were written into a 150 nm thick polymethylmethacrylate (PMMA) resist layer. The lateral distance between individual pattern arrays is 150 µm. After deposition of a 40 nm thick titanium layer, a lift-of process was used to produce the metallic structures on top of the sample with area filling factors between 0.5 and 0.15. These patterns were transferred into the QW structure by reactive ion etching (RIE).

During the RIE process the sample is exposed to a reactive gas plasma which contains active species that etch the material by chemical reactions. A CH_4/H_2 gas mixture (1:6 volume ratio) with a high frequency power of 90 W (corresponding to a DC bias of 450 V) at a pressure of 3.3 Pa (25 mTorr) is used for the II-VI compounds. The surface morphology and the lateral sizes of the etched structures were investigated by scanning electron microscopy (SEM). A typical SEM micrograph for small wires is shown in Fig. 1.

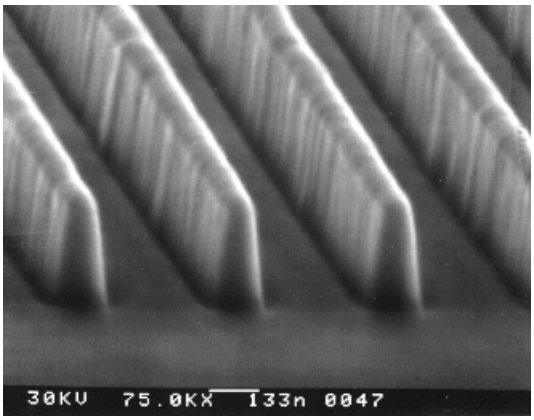

Fig. 1: Scanning electron microscopy image of CdZnSe/ZnSe wire structures defined by electron beam lithography and fabricated by reactive ion etching with a CH_4/H_2 gas mixture.

The damage which is introduced during RIE was also investigated by Auger electron spectroscopy (AES). For this purpose ZnSe, ZnTe, CdSe and CdTe epilayers were grown by molecular beam epitaxy and treated by reactive ion etching in CH_4/H_2 admixtures of different compositions and analyzed by AES with depth profiling. It was found that the CH_4:H_2 ratio has great influence on the chemical composition of the sample surface layer. For CH_4:H_2 ratios of about 1:7, the lowest deviation from stoichiometry and the lowest incorporation of oxygen and carbon was found [11].

Si substrates and Si/SiGe multiquantum well layers (Ge content: about 20%, 10 periods, Si layer width: 20.5 nm, and SiGe layer width of 1.8 nm) were laterally patterned using holographic lithography (λ = 458 nm) by reactive ion etching. The period of the wires is about 400 nm, the wire width about 200 nm. The etching depth is about 200 nm. The etching gases consisted of a mixture of SF_6 and CH_4 (90%/10% mixing ratio) using the following parameters. The rf-power was 30 Watt, the pressure 40 mTorr, the flowrate of SF_6 was 50 sccm, and for CH_4 it was about 2.5 sccm. (The corresponding parameters for the Si/SiGe MQW samples were the same). The remaining photoresist was taken off by an oxygen plasma. The surface morphology of the samples was investigated by scanning electron microscopy. The structural parameters were studied by different x-ray diffraction techniques, as described below.

3. Optical investigations

Low temperature (T = 1.9 K) PL measurements were performed with an x-y mapping set-up with a spatial resolution of 30 μm (determined by the laser spot diameter). The $Cd_{0.2}Zn_{0.8}Se$ QW embedded in ZnSe barriers (with a low temperature band gap E_g = 2.820 eV) was resonantly excited with an Ar^+ ion laser at an energy of 2.708 eV (457.9 nm) with about 100 W/cm^2. The PL spectra of the $Cd_{0.2}Zn_{0.8}Se$/ZnSe wires and dots with lateral dimensions between 80 and 1000 nm are shown in Fig. 2. The width of the PL emission line from the 2D reference mesa on the same sample is about 8 meV, a value which is essentially caused by alloy fluctuations in the ternary CdZnSe layer. Thus the splitting between free and bound excitons cannot be resolved.

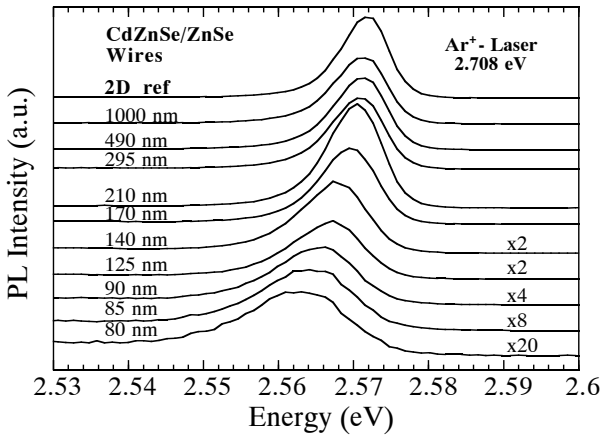

Fig. 2: Photoluminescence spectra of CdZnSe/ZnSe wire structures for lateral width of 80 to 1000 nm at 1.9 K. In addition the 2D quantum well reference spectrum on the same sample piece is shown.

Figure 3 shows the peak position of the PL line for wire and dot structures with lateral width between 80 and 1000 nm. A significant red shift occurs for wire sizes below 300 nm and dot sizes below 500 nm which is about 8 to 10 meV for the smallest wires and dots, respectively. The observed red shift will be discussed and compared with calculated band gap changes due to strain relaxation below.

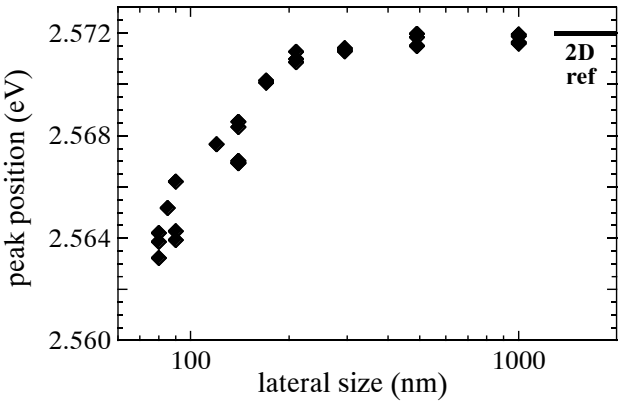

Fig. 3: Photoluminescence peak position of wire structures between 80 and 1000 nm for a resonant excitation energy of 2.708 eV (457.9 nm).

4. Strain Relaxation and Band-Gap Changes

Due to the formation of free perpendicular surfaces during the lateral patterning, the strained layers are able to relax partly. This is shown in Fig. 4 schematically for a thin wire structure. In order to calculate the detailed strain distribution of the wire structures, we follow an analytical method outlined by Faux and Haigh [3] but adopted it for our [110] oriented wires. This method solves the Airy stress equation by a Fourier series ansatz. The advantage of this method is that it is analytic, the disadvantage (as compared e.g. to finite element methods) is that only simple geometries can be treated with a restricted range of boundary conditions.

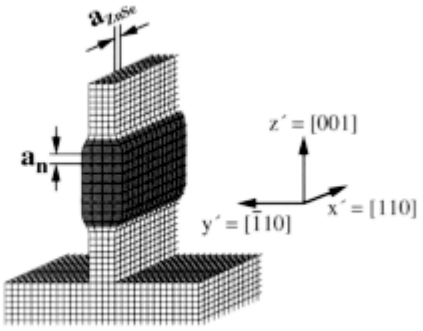

Fig. 4: Schematic strain relaxation of a laterally thin, partly relaxed CdZnSe/ZnSe wire.

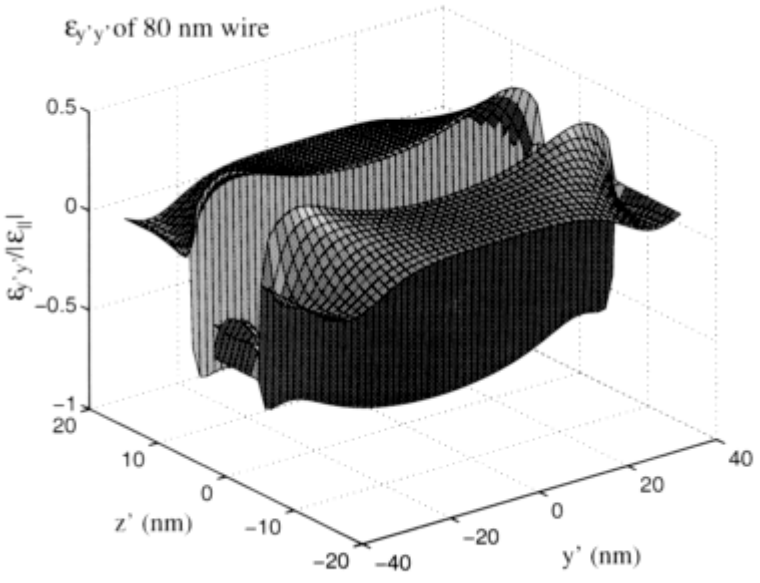

Fig. 5: Strain component $\varepsilon_{y'y'}$ for the wire cross section y´z with the y´ direction in the quantum well plane but perpendicular to the wire and the z direction along the growth direction.

Figure 5 shows the calculated strain distribution $\varepsilon_{y'y'}$, for a 80 nm wide wire of our CdZnSe/ZnSe structure, where the coordinate y´ in the epitaxial plane is perpendicular to the wires. The magnified displacements (by a factor 20) characterized by $\varepsilon_{y'y'}$ and ε_{zz} are shown in Fig. 6 for the wire cross section (the y´z-plane). It is clearly visible that the distortions are largest at the free surfaces. The shear component $\varepsilon_{y'z}$, which characterizes the deviations from a rectangular grid, is largest at the interface between the CdZnSe well and ZnSe barrier layers close to the free surface.

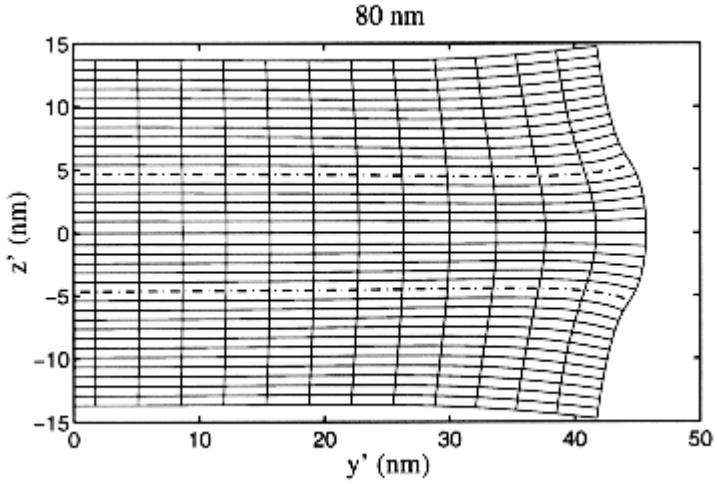

Fig. 6: The displacement, magnified by a factor 20, according to the strain components $\varepsilon_{y'y'}$ and ε_{zz} for the wire cross section (y´z-plane).

In <110> wires the non-uniform lattice deformation induces a piezoelectric polarization field [4], [5], [8]. The piezoelectric effect is directly connected with the shear components (shear strains ε_{jk}, $j \neq k$) as these describe the distortions of the cubic crystallographic cell. The potential distribution due to the piezoelectric were calculated accordingly for our wire structure with a width of 80 nm. The potential difference between upper and lower interface along the z-direction is about 12 meV. This bending of the quantum well potential and the associated electric field leads to a Stark effect which shifts the energy levels in the center of the well only by about 0.5 meV. Compared to the observed red shifts and the changes of the band gap due to deformation potential coupling, the effects due to piezoelectric coupling will be only important at still smaller wire structures.

Due to the lateral wire confinement by RIE patterning in 80 nm structures, the eigenstate energies inside the CdZnSe well change by less than 0.5 meV for electrons and 0.4 meV for heavy holes. These additional lateral confinement energies (blue shifts) are much smaller than the experimentally observed red shifts and will not give a relevant contribution.

The band gap changes due to the elastic strain relaxation in the wire structures are much more important. For the conduction band, the strain induced energetic shifts are easily calculated as no splitting of degeneracies due to a tetragonal or orthorhombic distortion of the lattice occurs. Only the hydrostatic component of the lattice affects the position of the CB edge [6]. The situation for the VB is more complicated as even in the 2D QW system (tetragonal distortion without the presence of shear strain components), the four-

fold degeneracy (Γ_8, including spin) of the cubic T_d crystal symmetry is removed. The energy levels of the valence band for cubic systems can be described by the k·p perturbation approach [7]. The effects of strain, confinement or other distortions can be included in the Hamiltonian of the system by using perturbation theory [10]. The deformation potential parameters a_v, b and d as introduced by Bir and Pikus [9] describe the energetic changes due to hydrostatic, tetragonal and shear deformations of the lattice, respectively. The solutions for the 6x6 Hamiltonian are obtained by numerical diagonalization for a given set of strain components which itself depends on the y´-z position inside the wire cross section. The resulting variation of the band gap over the cross section of the 80 nm wire is shown in Fig. 7.

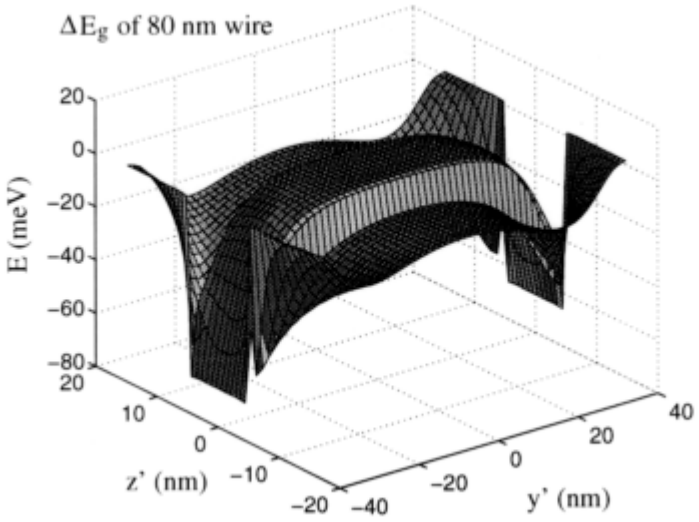

Fig. 7: Variation of the band-gap on the wire cross section (y´z-plane) for lateral wire width of 80 nm.

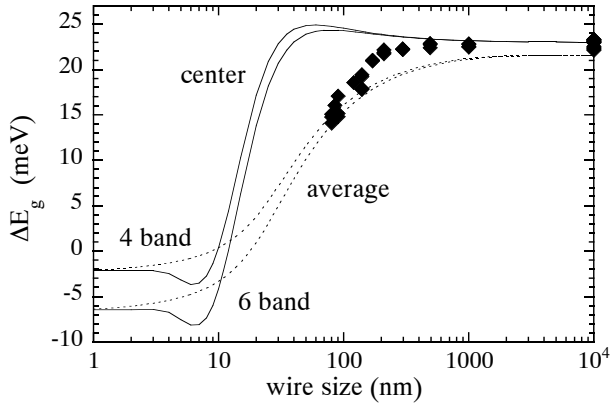

Fig. 8: Comparison of the calculated energy gap shift, averaged over the wire cross section, with the photoluminescence peak position for lateral wire width between 80 and 1000 nm. For comparison the gap in the center of the wire is shown for 6-band and 4-band calculation.

The calculated band gap changes of about 8 meV for the 80 nm wire structure are comparable with the experimentally observed PL line width of the 2D reference area on the sample. It is thus not expected to resolve any splitting of lines, but just a broadening and shift. It is also unknown how the PL emission efficiency is correlated with the spatial position in the wire structure. This efficiency depends on the RIE induced damage near the free surfaces as well as on the carrier diffusion after generation by incident laser beam. In Fig. 8 the calculated averaged energetic band gap shift is compared with the experimentally observed spectral red shift of the PL emission and gives a quantitative agreement.

5. X-Ray Investigations

The structural parameters of the Si/SiGe multiquantum well layers were studied by employing x-ray diffraction techniques, like double and triple crystal diffractometry. In Fig. 9a and b (311) ω-scans are shown for two Si-wire samples, with identical period (glancing angle exit diffraction). For the sample shown in Fig. 9a, the etching time was 13 min, for the sample shown in Fig. 9b it was 17 min. Since the number of wire satellites in Fig. 9b is somewhat larger, the structural quality of the periodic wire structures has certainly been improved.

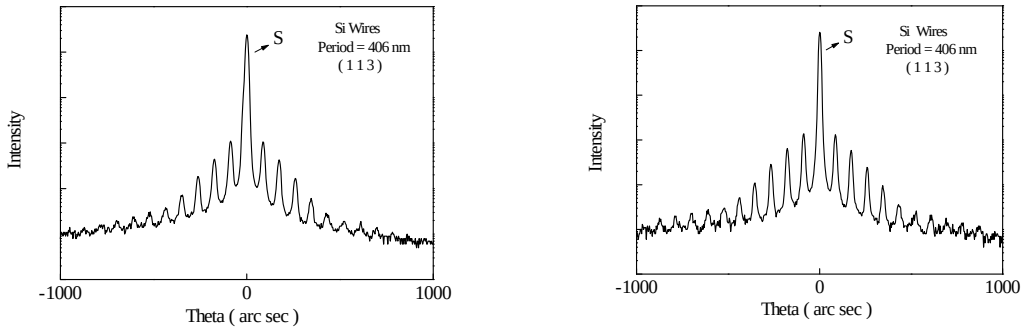

Fig. 9: ω-scans (113 reflection) of Si wire structures (area filling factor 0.5, period 406 nm) for RIE exposure times of 13 and 17 min, respectively)

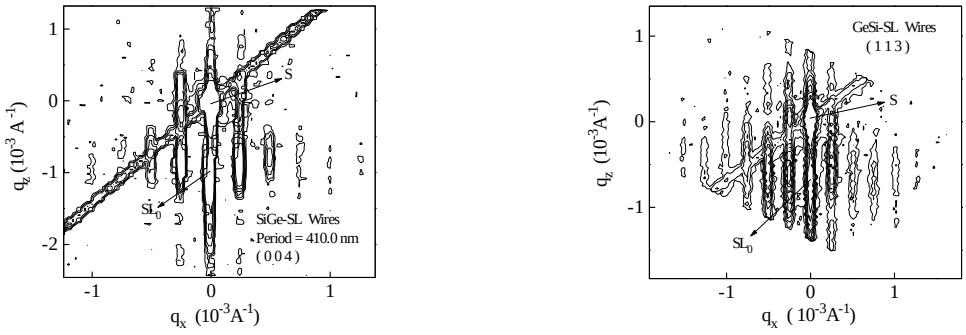

Fig. 10: (004) and (113) reciprocal space maps of a Si/SiGe wire structure (period 410 nm).

Reciprocal spacemaps around the (004) and the (311) reflection were recorded for the etched Si/SiGe multilayer samples (sample code: SiGe 46, which was grown by Stefan Zerlauth in the SiGeC MBE apparatus in Linz) as shown in Figs. 10a and 10b. Not only the MQW structure was etched through, but also part of the Si-buffer layer has been etched, as evidenced from the satellites accompanying the substrate peak marked by S. The MWQ structure gives rise to a superlattice peak (SL_O) which is accompanied along the q_X-direction by wire satellites. The period from the wire satellites is about 410 nm. A strain analysis based on these data will be performed.

References

[1] M.A. Haase, J. Qiu, J.M. DePuydt, H. Cheng, Appl. Phys. Lett. **59**, 1272 (1991).

[2] H. Jeon, J. Ding, W.R. Patterson, A.V. Nurmikko, W. Xie, D.C. Grillo, M. Kobayashi, R.L. Gunshor, Appl. Phys. Lett. **59**, 3619 (1991).

[3] D.A. Faux and J. Haigh, J. Phys. Condens. Matter 2, 10289 (1990).

[4] M. Grundmann, O. Stier and D. Bimberg, Phys. Rev. B 50, 14187 (1994).

[5] L. De Caro and L. Tapfer, Phys. Rev. B 51, 4374 (1995).

[6] C.G. Van de Walle, Phys. Rev. B **39** 1871 (1989).

[7] E.O. Kane in *Semiconductors and Semimetals*, Ed. R.K. Willardson and A.C. Beer, Vol. 1, Academic Press, New York 1966.

[8] L. De Caro and L. Tapfer, Phys. Rev. B 51, 4381 (1995).

[9] G.L. Bir and G.E. Pikus, in *Symmetry and strain induced effects in semiconductors*, John Wiley, New York 1974.

[10] J. Singh, in *Handbook on Semiconductors*, Ed. T.S. Moss, Vol. 2 by M. Balkanski, (Elsevier Science, Amsterdam 1994), p. 235ff; J. Singh, in *Physics of Semiconductors and their Heterostructures*, Ed. Anne T. Brown, (McGraw-Hill, Amsterdam 1993), p. 218ff.

[11] E. Wirthl, H. Straub, H. Sitter, G. Brunthaler, M. Schmid, D. Stifter, P. Bauer, "AES-Investigations of Plasma-Etched II-VI Binary Compounds", *Proceedings of the "International Symposium on Blue Laser and Light Emitting Diodes"*, Ohmsha Ltd., Tokyo 1996.